Proceedings of the ASME 2023 42nd International Conference on Ocean, Offshore and Arctic Engineering
OMAE2023
June 11-16, 2023, Melbourne, Australia

OMAE2023-105333

CURRENT EFFECT ON NONLINEAR WAVE HEIGHT

Arun Kumar
Civil Engineering Department
University of Dundee
Dundee, DD1 4HN, UK

Masoud Hayatdavoodi*
Civil Engineering Department
University of Dundee
Dundee, DD1 4HN, UK
&
College of Shipbuilding Engineering
Harbin Engineering University
Harbin, China
mhayatdavoodi@dundee.ac.uk

ABSTRACT

Interaction of uniform and shear currents with nonlinear waves is studied by use of the computational fluid dynamics approach. A range of nonlinear waves are considered including shallow- and deep-water waves, and the effect of currents of variable speed and direction on the wave height is investigated. Uniform current consists of a fixed horizontal velocity across the water depth, while shear current imposes a linearly varying velocity from the seafloor to the still-water level. The current speeds are selected such that they remain comparable with the horizontal particle velocity under the wave crest and wave trough. A computational wave-current tank is developed for this purpose and the combined wave-current condition is obtained by developing a new wave-current maker in an open-source computational fluid dynamics package, namely OpenFOAM. The model is tested against laboratory measurements of various types of wave and currents and very good agreement is observed. The model is then used to investigate how currents of different profile, speed and direction modify the wave field. While the focus of the study is on the effect of these currents on the change of wave height, the surface elevation of the waves is also assessed in some cases. Discussion is provided on the differences between current effect on the wave height of shallow-water waves vs deep-water waves. The wave nonlinearity is found to play a remarkable role on how the wave changes under the ambient current. Shear currents are observed to have a stronger influence on the change of wave height than uniform currents.

Keywords: Wave-current interaction, nonlinear waves, wave-current tank, uniform current, shearing current

1 INTRODUCTION

The presence of currents strongly influences ocean wave characteristics. In particular, the change of wave height, H, is of interest, as this modifies the loads imparted by the wave-current system onto coastal and offshore structures. Different current profiles are observed at various geographic locations [1–5], and this affects the resulting wave-current interaction. The movement of sediment on the seabed, the evolution of coastal morphology as well as the movement of the pollutants are affected by the presence of ambient currents, see [6,7]. Study conducted by Liau et al. [8] found that the wave refraction and diffraction from an uneven seafloor is influenced by wave-current interaction. The presence of currents introduces significant drag forces and modifies the total load generated by the wave-current field, see [9]. Toffoli et al. [10] reported that the presence of an opposing current (i.e., wave and current propagating in opposite directions to each other) can lead to instability and breaking of wave packets. Hence, a study of wave-current interaction is imperative to ocean

*Address all correspondence to this author.

engineering applications.

The change of wave height has been investigated experimentally in several studies. Typically, currents that (i) have a fixed horizontal velocity across the water depth, h, or (ii) have a varying velocity from the seafloor to the still-water level (SWL) are chosen. Experiments conducted by Brevik & Bjørn [11] and Brevik [12] investigating the interaction of waves with following (currents propagating in the same direction as the waves) and opposing currents indicate that, in case of following current, wave height decreases, whereas, in case of opposing current, wave height increases. The studies considered rippled and smooth seabeds but were confined to deep water conditions. Wave height was observed to be increasing in the experimental study conducted by Thomas [13], as linear waves interacted with non-uniform opposing currents. Similar behaviour in change of wave height was observed in a follow-up experimental investigation conducted by Thomas [14], where nonlinear waves were considered. These studies, too, were limited to deep water conditions. The effect of following and opposing currents with a mixed profile (i.e., maintaining a uniform profile up to a certain depth and then changing linearly with water depth) on nonlinear deep water waves was investigated experimentally by Swan et al. [15]. It was observed that wave height decreases with following current and increases with opposing current. The interaction between waves and a uniform current was assessed experimentally by Umeyama [16] focusing on particle velocities and trajectories. They concluded that the wave height in case of following current was 13% to 17% smaller than the wave-only condition. Several other studies have experimentally investigated the interaction between waves and currents, see e.g., [17–20].

A numerical study investigating the effect of uniform currents on near-resonant triad interactions of gravity waves in shallow water was conducted by Chen et al. [21]. The numerical wave tank was set up using Boussinesq-type equations for the fully coupled wave-current interactions. The first order wave height was observed to decrease with following currents and increase with opposing currents and the study was limited to one current profile. Numerical investigation of the interaction between a linear shear current and a strongly nonlinear solitary wave in shallow water conducted by Choi [22], indicated that a solitary wave narrows down when interacting with a following current and widens when facing an opposing current. A numerical model based on the Reynolds-Averaged Navier–Stokes (RANS) equations was used by Zhang et al. [23], to investigate the interaction of a solitary wave with following and opposing uniform currents. Following current was found to decrease the wave height while opposing current increased it. The effect of a linear shear current on solitary waves in shallow water was numerically studied by Guyenne [24], using a two-dimensional direct numerical simulation method and the wave height was found to be larger in case of opposing currents and smaller in case of following currents. Other numerical investigations of wave-current interactions include [25–30].

A numerical investigation conducted by solving the Navier-Stokes (NS) equations for the case of regular waves in shallow water (generated using Cnoidal wave theory) interacting with following and opposing currents of different profiles was conducted by Kumar & Hayatdavoodi [31]. Several waves were considered and it was observed that in case of following currents, the wave height increased and in case of opposing current, the wave height reduced. This was observed to be a peculiar behaviour in change of wave height and merited further investigation. From the assessment of the literature, it was also observed that a study of the interaction between regular waves in shallow water and different current profiles was missing. Hence, the goal of this study is to further investigate the interaction of regular waves in shallow and deep waters with currents of different profiles and assess their effect particularly on the change of wave height.

The theory associated with the computational approach used in this study and the steps taken to solve the governing equations are discussed first. Then, a description of the numerical wave-current tank, the mesh setup and the layout of the numerical sensors is provided. This is followed by a discussion about the different waves and current profiles chosen for the study. Then, the results of the numerical wave-current tank are compared with experimental studies, and the results of the wave-current study on change of wave height along with the major inferences are discussed. Lastly, some concluding remarks about the results are provided.

2 THEORY AND NUMERICAL SOLUTION

A two-dimensional Cartesian coordinate system with the positive $x-$direction pointing to the right and the positive $z-$direction pointing against the acceleration due to gravity is chosen. The waves propagate along the positive $x-$direction and the origin of the coordinate system is fixed at the SWL. The fluid is incompressible, Newtonian and homogeneous substance at the scale of observation. It is assumed that the effect of turbulence in case of wave-current interaction over a flat seafloor is negligible, see e.g., [30, 32, 33] for numerical studies that use laminar flow assumption in case of wave-current interaction. The fluid pressure and velocity are considered differentiable in space and time. The flow is governed by the mass and momentum conservation equations,

$$\vec{\nabla}.\vec{V} = 0, \tag{1}$$

$$\frac{\partial \vec{V}}{\partial t} + \nabla\vec{V}.\vec{V} = -\frac{1}{\rho}\nabla p + \nu\vec{\nabla}^2\vec{V} - \vec{g}, \tag{2}$$

where $\overrightarrow{V} = u_x \overrightarrow{i} + u_z \overrightarrow{k}$ is the velocity vector, $\overrightarrow{i}$ and $\overrightarrow{k}$ are the unit normal vectors in $x-$ and $z-$ directions, respectively, t is time, ρ is the density of the fluid, p is the pressure, ν is the kinematic viscosity and $\overrightarrow{g}$ represents the body force vector due to gravity. The gradient function is represented by ∇, while the divergence and Laplacian vectors are represented by $\overrightarrow{\nabla}$ and $\overrightarrow{\nabla}^2$, respectively. Equations (1) and (2) are solved simultaneously for both air (on top) and water phases. The free surface between air and water is captured using the Volume of Fluid method, see [34]. The equations are only solved in the $x-$ and $z-$ directions in this two-dimensional study.

The pressure-velocity coupling problem is iteratively solved using the PIMPLE algorithm, see [35]. The governing equations are discretized using finite volume approach. An open source computational fluid dynamics package, OpenFOAM, is used to solve the computational domain.

The shallow water wave in this study is generated using the Cnoidal wave theory. Starting from the Korteweg–de Vries (KdV) equation, the surface elevation, η, is obtained as

$$\eta = \eta_{min} + Hcn^2(\theta, m), \tag{3}$$

where, η_{min} is the distance between the wave trough and the SWL and cn represents the Jacobian elliptic function of variables θ and m $(0 \leq m < 1)$ ([36]). η_{min} is defined as

$$\eta_{min} = \left(\frac{1}{m}\left(1 - \frac{E}{K}\right) - 1\right) H, \tag{4}$$

where, $K = K(m)$ and $E = E(m)$ are the complete elliptical integrals of the first and second kind, respectively. The variable θ, in Eq. (3), is defined as

$$\theta = 2K\left(\frac{t}{T} - \frac{x}{\lambda}\right). \tag{5}$$

The horizontal particle velocity according to the Cnoidal wave theory is given as

$$u_{x(w)} = c\left[\frac{\eta}{h} - \left(\frac{\eta}{h}\right)^2 + \frac{1}{2}\left(\frac{1}{3} - \left(\frac{z+h}{h}\right)^2\right) h\eta_{xx}\right], \tag{6}$$

where, c is the phase velocity, z is the vertical coordinate that varies from 0 to $-h$ and η_{xx} is obtained by differentiation of Eq. (3).

The deep water wave is generated using the Stream Function wave theory which provides a nonlinear solution to the steady wave problem in arbitrary depth, see [37, 38]. Here, the horizontal particle velocity is given as

$$u_{x(w)} = \left(\frac{\omega}{k} - \overline{u}\right) + \sum_{j=1}^{n} jB_j \frac{\cosh jk(z+h)}{\cosh jkh} \cos j(kx - \omega t + \phi), \tag{7}$$

where, ω is the wave frequency given as $2\pi/T$, k is the wave number, $\overline{u}$ is the mean fluid speed, B_j are dimensionless constants, z is the vertical coordinate, x is the horizontal coordinate and ϕ is the wave phase angle.

Hereafter, acceleration due to gravity (g), density of water (ρ) and the water depth (h), are employed as the dimensionally independent set used to nondimensionalize all parameters. Therefore, $\overline{H} = H/h$, $\overline{\eta} = \eta/h$, $\overline{T} = T/\sqrt{h/g}$, $\overline{u_x} = u_x/\sqrt{gh}$ and $\overline{\lambda} = \lambda/h$. The bar over the variables is removed from all dimensionless quantities for simplicity.

A theoretical wave-current maker is used to set up the combined wave-current field. The horizontal particle velocity at the wave-current maker is obtained by the linear superposition of the wave and the current velocities. Hence, the wave-current horizontal particle velocity, $u_{x(wc)}$, for the combined current and wave, at the wave-maker, is given by

$$u_{x(wc)} = u_{x(w)} + u_c, \tag{8}$$

where, $u_{x(w)}$ is the horizontal particle velocity due to the wave given in Eqs. (6) and (7), while u_c is the horizontal particle velocity due to the current.

The numerical wave-current tank comprises of three regions: (i) the region where the horizontal and vertical particle velocities, pressure field and free surface elevation are enforced according to the theoretical wave-current setup, (ii) the computational region where the NS equations are solved iteratively, and (iii) the region where the wave-current system is allowed to dissipate gradually, namely the wave-current absorption zone. The wave-current generation and absorption zones (regions (i) and (iii)), are also known as the inlet and outlet relaxation zones respectively. The relaxation zones proposed by [39] for waves have been modified to incorporate the current. The outlet relaxation zone minimises the computational cost by restricting the length of the numerical domain. The current profile linearly superposed at the wave generation zone is replicated at the boundary of the outlet relaxation zone in order to conserve mass in the domain. The fluid velocity at the flat, stationary tank bottom is set to 0, i.e. a no-slip boundary condition is used on this boundary. The change in mass of water in the tank over time has been continuously monitored for all computational investigations carried out

in this study. It is observed that the change in mass of water in the tank is always less than 0.7%.

3 NUMERICAL TANK SETUP

The setup of the numerical wave-current tank and its computational mesh are discussed in this section. A structured, hexahedral mesh is used for the spatial discretization of the numerical domain. Mesh refinement is defined on the basis of the wavelength, λ, and wave height of the incident wave. The mesh configuration here follows the mesh convergence study of Kumar & Hayatdavoodi [31] for a similar wave-current tank, where increasing number of cells per wavelength and wave height are considered. A mesh with 62 cells per wave height and 500 cells per wavelength is chosen as it is found to be optimum and computationally reasonable for the cases considered here.

The two-gauge method outlined by Grue [40] is employed to monitor the wave reflection at the centre of the domain. This method has been previously employed by Hayatdavoodi et al. [41] to obtain the reflection and transmission coefficients of strongly nonlinear waves. The variation of the reflection coefficient with time is studied and it is found that the reflection from the outlet relaxation zone remains below 2%.

A numerical domain with a wave-current generation zone of length λ and a wave-current absorption zone of length 0.75λ results in a stable and efficient wave-current tank, with negligible reflection from the open boundary, as noted in Kumar & Hayatdavoodi [42]. This is in agreement with the previous investigations of Hayatdavoodi et al. [43] on the optimum computational domain length for nonlinear waves. The total length of the numerical wave tank is 7λ, ensuring that at least five waves are entirely outside the relaxation zones for the investigations at all times. The schematic of the numerical wave tank along with the location of the wave gauges is shown in Fig. 1. Surface elevation is recorded by Gauges GI and GII, placed at distances λ and 2λ from the inlet relaxation zone, respectively.

4 WAVE-CURRENT CONDITIONS

The waves and currents chosen in this study are discussed in this section. This study considers two nonlinear waves propagating in, (i) shallow and (ii) deep water in the presence of ambient currents. The water depth is fixed at 0.15 m (except for cases used in comparisons) and the wave parameters are altered to move from shallow water wave to deep water wave. The wave parameters are described in Table 1. Wave W1 is the shallow water wave generated using the Cnoidal wave theory (with steepness = 0.008, h/gT^2 = 0.001 and H/gT^2 = 0.0003) and wave W2 is the deep water wave generated by the use of Stream function wave theory (with steepness = 0.0216, h/gT^2 = 0.1112 and H/gT^2 = 0.004).

Two current profiles are considered in this study, namely a uniform current profile and a shear current profile. The horizontal particle velocity due to the current, u_c, is a function of the vertical coordinate, and it is defined as $u_c(z) = (z+1)\,u_{sc}$, for the shear current, while it is fixed at $u_c(z) = u_{uc}$, for the uniform current. Here, u_{sc} is the current velocity at the free surface, in case of shear current and u_{uc} is the current velocity at the free surface, in case of uniform current. The current velocities are chosen such that they remain comparable with the horizontal particle velocities due to the waves of this study. This is observed in Fig. 2, which shows the horizontal particle velocity profile under the wave crest for both waves of the study along with the currents chosen in these investigations. These horizontal particle velocities are only imposed at the inlet and outlet relaxation zones. In total, 18 current configurations are considered in this study by changing the current profile, magnitude and direction relative to the direction of wave propagation and Table 1 provides details of the selected current profiles. Here, a following current is represented by a positive current velocity and an opposing current is represented by a negative current velocity.

The interaction of waves W1 and W2 with all current configurations is investigated in this study. Along with the two wave-only computations, this results in a total of 38 wave- & wave-current computations. The results of these wave-current interaction cases are then used to investigate the variation of surface elevation and the change of wave height with increasing current velocities and changing current direction.

5 RESULTS AND DISCUSSION

The results of the numerical wave-current tank are discussed in this section. First, results of the NS model are compared with existing laboratory experiments and other computational studies. Then, the wave-current interaction computations are carried out and the changes in surface elevation and the change of wave height are investigated.

5.1 Comparison with Laboratory Experiments

The numerical wave-current is used to set up a coexisting wave-current field and the results are compared with the laboratory measurements and numerical assessments performed by Chen et al. [44]. They also used the higher-order boundary element method (HOBEM) based on potential flow theory to solve the computations. In these experiments, a wave with H = 0.083 and T = 4.044 propagates over a uniform current with u_{uc} = 0.0824 in a tank with h = 0.6 m. Time series of surface elevation of the wave-current field, recorded by a gauge located at distance λ from the inlet relaxation zone (GI), is shown in Fig. 3. Results of the NS model show good agreement with the computations and laboratory measurements of Chen et al. [44].

Results of the NS model, for the wave-current cases con-

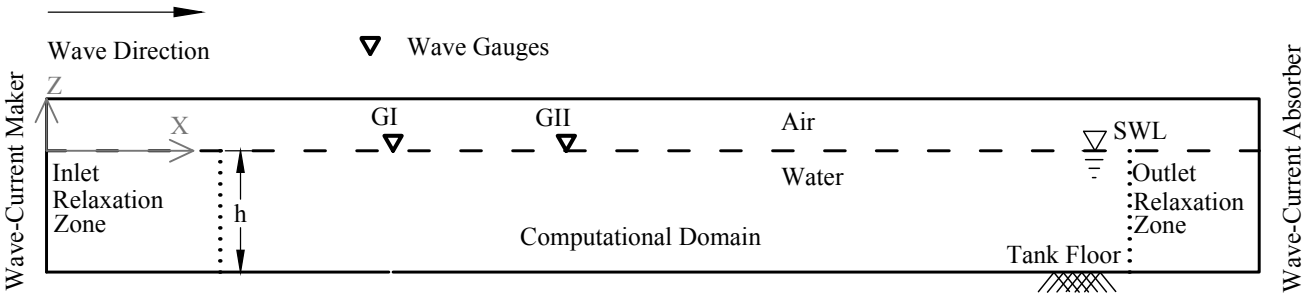

FIGURE 1. SCHEMATIC OF THE NUMERICAL WAVE-CURRENT TANK ALONG WITH THE WAVE GAUGES.

TABLE 1. WAVE-CURRENT CONDITIONS CONSIDERED IN THIS STUDY.

Wave	Wave height	Wave period	Current type	Current velocity at the free surface
W1	0.2	24.99	Uniform	±0.0022
				±0.035
				±0.0701
				±0.105
				±0.14
				±0.175
			Shear	±0.035
				±0.0701
				±0.105
W2	0.036	2.99	Uniform	±0.0022
				±0.035
				±0.0701
				±0.105
				±0.14
				±0.175
			Shear	±0.035
				±0.0701
				±0.105

sidered here, are presented and discussed in the following sub-sections. First, surface elevation is analysed as the waves interact with different currents. This is followed by the study of change of wave height. Each sub-section is further categorized based on the type of current interacting with the waves.

5.2 Surface Elevation

The surface elevation of the incident waves as they interact with different currents is investigated in this section. Figure 4 depicts the time series of surface elevation recorded at Gauges GI and GII in the absence of current along with the analytical solution for surface elevation obtained using the Cnoidal wave theory, Eq. (3), and the analytical solution for surface elevation obtained using Stokes Second wave theory (valid for the selected

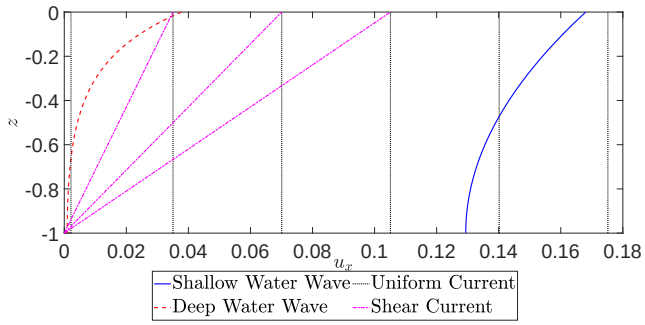

FIGURE 2. THE IMPOSED HORIZONTAL PARTICLE VELOCITY PROFILES SHOWN FOR THE FOLLOWING CURRENT CASES AND UNDER THE CREST OF THE WAVE CASES. THE CURRENT PROFILES ARE MIRRORED ALONG THE VERTICAL AXIS WITH RESPECT TO $u_x = 0$, IN THE CASE OF OPPOSING CURRENTS.

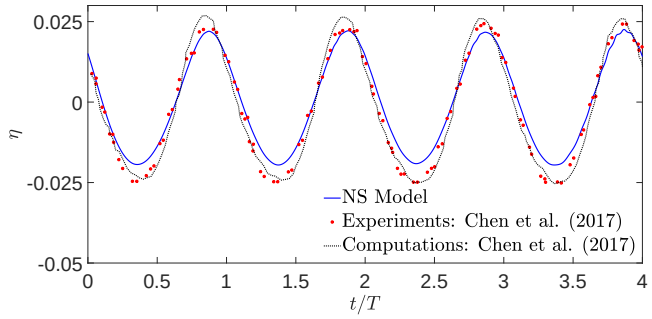

FIGURE 3. TIME SERIES OF SURFACE ELEVATION UNDER THE WAVE-CURRENT SYSTEM OBTAINED USING THE NS MODEL, COMPARED WITH LABORATORY MEASUREMENTS AND COMPUTATIONS OF CHEN ET AL. [44], $H = 0.083$, $T = 4.044$, $h = 0.6$ m AND $u_{uc} = 0.0824$.

wave and an alternative to the Stream Function wave theory used in the computations). It is observed that the waves generated in the tank are in good agreement with the respective analytical solutions. This is followed by introduction of currents into the domain and the surface elevation is studied in their presence. The change in surface elevation is investigated by defining the change of the peak of surface elevation, $\eta' = [(\eta_{wc} - \eta_w)/\eta_w] \times 100$, where η_{wc} is the peak of surface elevation in the presence of the current and η_w is the peak of surface elevation from the wave-only case. Therefore, η' represents the percentage change of peak of surface elevation due to the presence of currents. In order to obtain the peak of surface elevation at a given gauge, all waves in the time series of surface elevation (excluding the ramp wave) are observed, the highest and lowest peaks are discarded and the mean of the remaining peaks in the signal is used for the assessment.

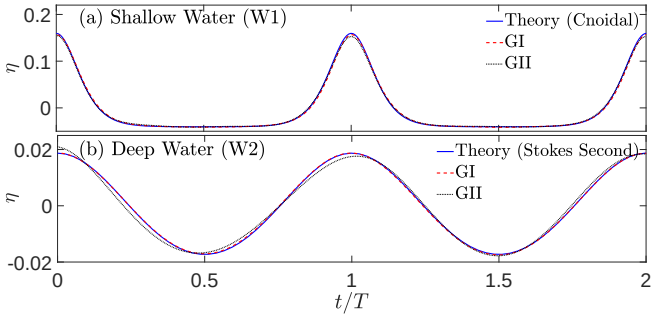

FIGURE 4. TIME SERIES OF SURFACE ELEVATION RECORDED AT GAUGES GI & GII FOR WAVES (a) W1 AND (b) W2, IN THE ABSENCE OF CURRENT.

The change in peak of surface elevation as shallow and deep water waves interact with following and opposing uniform currents is shown in Fig. 5. It is observed that in case of deep water wave-current interaction, a following current decreases η' and an opposing current increases it. Opposing current has a stronger effect on the change in peak of surface elevation (up to 20%) than following current (up to 8%). In case of shallow water wave-current interaction, it is found that following current increases the peak of surface elevation, while an opposing current reduces the same. η' is found to change almost linearly with increasing current velocities.

The effect of following and opposing shear currents on the change in peak of surface elevation is shown in Fig. 6. As observed with uniform current, in case of shallow water wave-current interaction, following current increases η' while opposing current decreases the same. Shear currents have a stronger influence on η' (up to $\pm 11\%$) when compared with uniform currents (up to $\pm 6\%$). In case of deep water wave-current interaction, it is observed that following current reduces η', however, as the shear current velocity increases, η' also increases. Opposing shear currents increase peak of surface elevation, with the strongest shear current increasing η' by 17%.

5.3 Change of Wave Height

In this section, the change of wave height of the incident wave due to the presence of currents is studied. There are two methods that are employed to study the change of wave height.

The first method uses the snapshots of the surface elevation recorded within the domain (outside the relaxation zones) at a given time. The change of wave height is then assessed statistically by measuring the peak-to-peak variation of wave height. Similar to the approach adopted in case of surface elevation, the maximum and minimum values of wave height are rejected and an arithmetic mean of the remaining wave height data is considered to obtain a statistically sound data set.

The second method assesses the change of wave height by

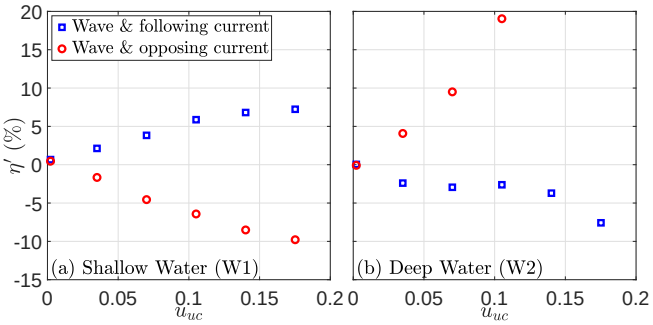

FIGURE 5. CHANGE IN SURFACE ELEVATION AS WAVES IN (a) SHALLOW WATER AND (b) DEEP WATER, INTERACT WITH FOLLOWING AND OPPOSING UNIFORM CURRENTS.

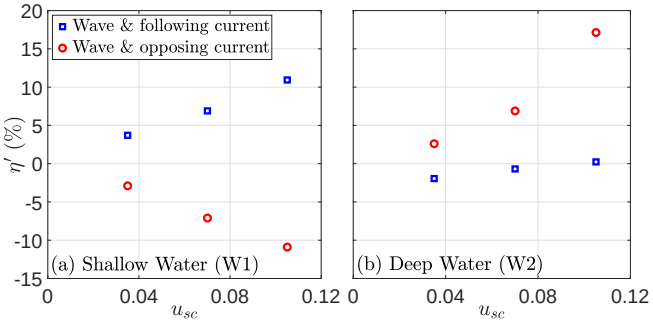

FIGURE 6. CHANGE IN SURFACE ELEVATION AS WAVES IN (a) SHALLOW WATER AND (b) DEEP WATER, INTERACT WITH FOLLOWING AND OPPOSING SHEAR CURRENTS.

reconstructing the snapshots of the surface elevation recorded within the domain (outside the relaxation zones) at a given time, using the Fourier series as:

$$\eta(x,t_0) = \sum_{i=1}^{n} A_i cos(k_i x + \delta_i), \tag{9}$$

where the surface elevation, η, is presented as a function of the $x-$coordinate at a given time, t_0, see e.g., [45]. Here, A_i are the amplitudes of the first ($i = 1$) and higher ($i > 1$) harmonics, while k_i and δ_i represent the spatial frequency and phase angle, respectively. In this approach of wave height assessment, only the amplitudes corresponding to the first and second harmonics ($i = 1$ and $i = 2$, respectively) are considered. A sample case of wave height assessment conducted with this method is portrayed using the Fourier transform output in Fig. 7. Here, the Fourier transform of the snapshots of wave W1 and W2 interacting with following and opposing uniform currents of magnitude, u_{uc} = 0.035, is presented. It is observed that the shallow water wave is highly nonlinear as the amplitude of the first and second

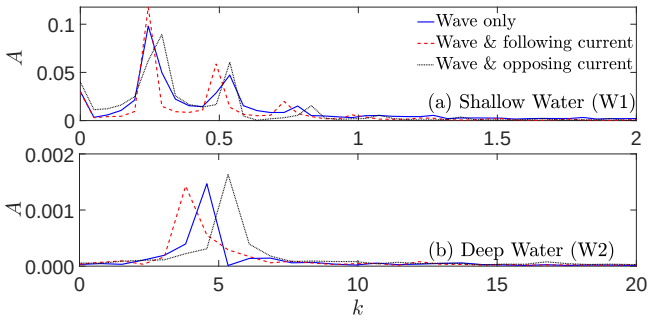

FIGURE 7. FOURIER TRANSFORM OF THE SURFACE ELEVATION OF WAVES (a) W1 AND (b) W2 IN THE DOMAIN AT t = 10T, AS THEY INTERACT WITH FOLLOWING AND OPPOSING UNIFORM CURRENTS, $u_{uc} = \pm 0.035$.

harmonics are significant. However in case of deep water wave, only the amplitude of the first harmonic is significant. Therefore in case of deep water wave, discussion hereafter is limited to the first harmonic components, while both first and second harmonic components are assessed while investigating the shallow water wave.

In the first method, the changes in wave height are defined using $H' = [(H_{wc} - H_w)/H_w] \times 100$, where H_{wc} is the height of the wave under the influence of current and H_w is the height of the wave in the absence of current. Hence, this parameter represents the percentage change in wave height due to the presence of currents. This technique is also utilised to study the change of the peak of surface elevation in the previous section, see Sec. 5.2. Under the second method, the changes in wave height are defined using $H'_i = [(H_{i(wc)} - H_{i(w)})/H_{i(w)}] \times 100$, where $H_{i(wc)}$ is the wave height of the ith harmonics of the wave in the presence of current and $H_{i(w)}$ is the wave height of the ith harmonics of the wave in the absence of current.

5.3.1 Uniform Current The effect of uniform currents on the wave height of shallow and deep water waves is studied in this section. The change of wave height as both waves interact with following and opposing uniform currents of increasing magnitudes is shown in Fig. 8. The behaviour of H' as the shallow water wave interacts with uniform currents is quite peculiar, as observed in Fig. 8(a). It is found that following currents consistently increase the wave height of the shallow water wave and opposing currents reduce the same. Stronger currents have a more significant impact of the change of wave height. It is inferred that the nature of the incident wave plays a decisive role in shaping the outcome of change of wave height as waves interact with following and opposing uniform currents.

It is seen that in deep water conditions, a following current decreases the wave height while an opposing current increases the wave height. This is in agreement with the trend observed in

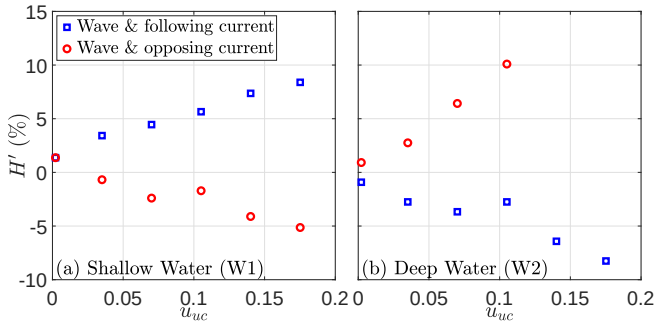

FIGURE 8. CHANGE OF WAVE HEIGHT AS WAVES IN (a) SHALLOW WATER AND (b) DEEP WATER, INTERACT WITH FOLLOWING AND OPPOSING UNIFORM CURRENTS.

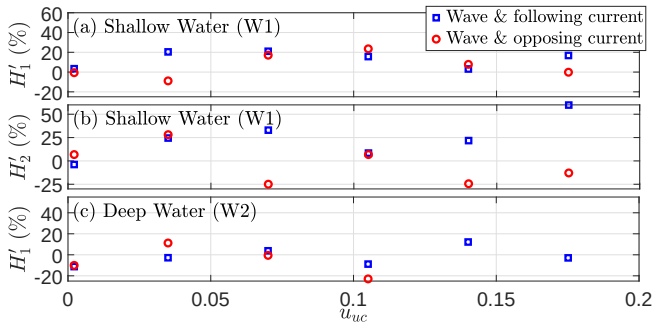

FIGURE 9. CHANGE OF WAVE HEIGHT OF THE (a) FIRST AND (b) SECOND HARMONIC OF THE SHALLOW WATER WAVE, AND (c) FIRST HARMONIC OF THE DEEP WATER WAVE, AS THEY INTERACT WITH FOLLOWING AND OPPOSING UNIFORM CURRENTS.

literature. The change in H' also increases with the current velocity. In case of wave interaction with opposing current in deep water conditions, it is observed that the wave is unable to propagate through the domain for current velocities larger than 0.105. Hence, there are only four data points available for discussion when wave W2 interacts with uniform opposing currents, as observed in Fig. 8(b).

The results of wave height assessment conducted with the second method are shown in Fig. 9. Figures 9(a) & 9(b) indicate that the effect of currents on the nonlinear components of the incident waves is significant. H_2' is observed to behave quite differently from H_1' in these figures. The effect of current direction on the change of wave height of the first harmonic appears to be insignificant. For the deep water wave-current interaction, it is observed that in case of opposing currents, H_1' initially increases and then decreases. In case of following currents, H_1' remains largely negative at all current speeds.

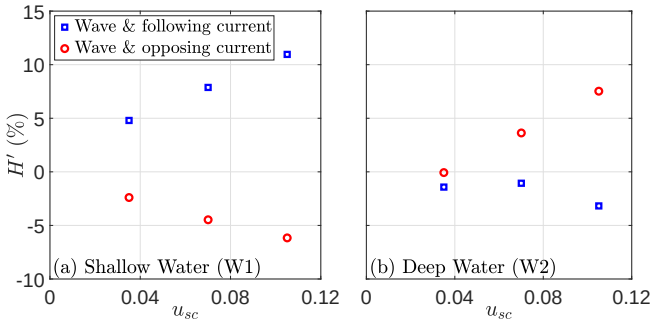

FIGURE 10. CHANGE OF WAVE HEIGHT AS WAVES IN (a) SHALLOW WATER AND (b) DEEP WATER, INTERACT WITH FOLLOWING AND OPPOSING SHEAR CURRENTS.

5.3.2 Shear Current The change of wave height as shallow and deep water waves interact with following and opposing shear currents is discussed here. The change of wave height as both waves interact with following and opposing shear currents of increasing magnitudes is shown in Fig. 10. In Fig. 10(a) it is observed that in case of shallow water wave-current interaction, following current increases the wave height while opposing current reduces it. Shear currents are also observed to be nearly twice as influential on H' when compared with uniform currents with the same free surface velocity. Further, it is seen that following shear current has a stronger effect on H' than opposing shear current. In case of deep water wave-current interaction, following shear currents are observed to reduce H', while opposing shear currents increase it. Following shear currents weakly influence the change of wave height in deep water waves, when compared with uniform currents. Opposing shear currents have stronger influence on H', when compared to following shear currents, but they are still weaker than opposing uniform currents in deep water. This indicates that shear currents have a greater influence on the wave height than uniform currents in case of shallow water waves, whereas the effect of uniform currents is more significant in deep water waves.

The assessment of wave height is carried out using the Fourier analysis method and its results are shown in Fig. 11. Figures 11(a) & 11(b) indicate that the nonlinear components of the incident waves are significantly influenced by the shear currents. In case of shallow water wave-current interaction, H_1' increases with following shear current by 20%. H_1' initially decreases with opposing current (-20%), but increases with stronger shear currents. H_2' is not influenced by the direction of shear currents, as both following and opposing currents increase H_2'. In case of deep water wave-current interactions, both following and opposing shear currents generally reduce H_1'.

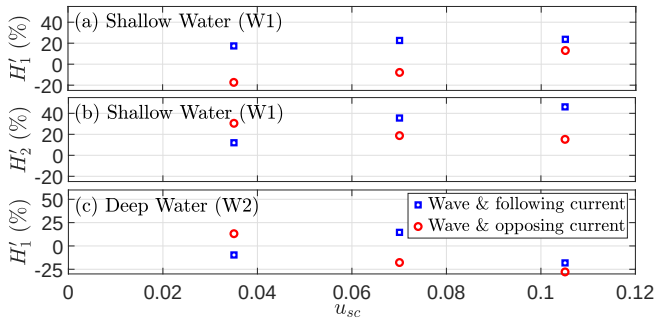

FIGURE 11. CHANGE OF WAVE HEIGHT OF THE (a) FIRST AND (b) SECOND HARMONIC OF THE SHALLOW WATER WAVE, AND (c) FIRST HARMONIC OF THE DEEP WATER WAVE, AS THEY INTERACT WITH FOLLOWING AND OPPOSING SHEAR CURRENTS.

6 CONCLUSION

The effect of uniform and shear currents on nonlinear waves is studied by use of a numerical wave-current tank. Waves propagating in both, shallow water and deep water are considered, as they interact with following and opposing currents of different magnitudes.

It is observed that in case of deep water wave-current interactions, a uniform following current reduces the wave height, while a uniform opposing current increases the same. An opposing current is found to have a more significant effect on the change of wave height. In case of shallow water wave-current interaction, however, it is found that a uniform following current increases the wave height, while a uniform opposing current reduces it. The change of wave height is observed to be larger when waves interact with currents of higher velocities. A similar response is also observed from the change of peak of surface elevation. Current velocities and direction do not strongly influence the first harmonic of the incident waves.

In shallow waters, following shear currents increase the wave height while opposing shear currents decrease it and the reverse is observed in deep waters. It is also seen that shear currents have a stronger influence on H' in shallow waters, when compared with uniform currents of the same free surface velocity. This indicates that the current velocity near the free surface plays a more significant role here than the current velocity at points further away from it. In case of deep water waves, uniform currents have a stronger influence on H', than shear currents with the same free surface velocity.

REFERENCES

[1] Jeans, G., Grant, C., and Feld, G., 2003. "Improved current profile criteria for deep-water riser design". *Journal of Offshore Mechanics and Arctic Engineering,* ***125***(4), pp. 221–224.

[2] Carollo, C., Astin, I., and Graff, J., 2005. "Vertical structure of currents in the vicinity of the Iceland-Scotland ridge". *Annales Geophysicae,* ***23***(6), pp. 1963–1975.

[3] Shen, C. Y., Evans, T. E., Mied, R. P., and Chubb, S. R., 2008. "A velocity projection framework for inferring shallow water currents from surface tracer fields". *Continental Shelf Research,* ***28***(7), pp. 849–864.

[4] Sheikh, R., and Brown, A., 2010. "Extreme vertical deep-water current profiles in the South China Sea, Offshore Borneo". In International Conference on Offshore Mechanics and Arctic Engineering, pp. 585–595, Shanghai, China. 06/06/2010–11/06/2010.

[5] Jeans, G., Prevosto, M., Harrington-Missin, L., Maisondieu, C., Herry, C., and Lima, J. A. M., 2012. "Deep-water current profile data sources for riser engineering offshore Brazil". In International Conference on Offshore Mechanics and Arctic Engineering, pp. 155–168, Rio de Janeiro, Brazil. 01/07/2012–06/07/2012.

[6] Soulsby, R. L., Hamm, L., Klopman, G., Myrhaug, D., Simons, R. R., and Thomas, G. P., 1993. "Wave-current interaction within and outside the bottom boundary layer". *Coastal Engineering,* ***21***(1-3), pp. 41–69.

[7] Tao, J., and Han, G., 2002. "Effects of water wave motion on pollutant transport in shallow coastal water". *Science in China Series E: Technological Science,* ***45***(6), pp. 593–605.

[8] Liau, J. M., Roland, A., Hsu, T. W., Ou, S. H., and Li, Y. T., 2011. "Wave refraction-diffraction effect in the wind wave model WWM". *Coastal Engineering,* ***58***(5), pp. 429–443.

[9] Markus, D., Wüchner, R., and Bletzinger, K. U., 2013. "A numerical investigation of combined wave-current loads on tidal stream generators". *Ocean Engineering,* ***72***, pp. 416–428.

[10] Toffoli, A., Waseda, T. H. T. K. D., Houtani, H., Kinoshita, T., Collins, K., Proment, D., and Onorato, M., 2013. "Excitation of rogue waves in a variable medium: An experimental study on the interaction of water waves and currents". *Physical Review E,* ***87***(5), p. 051201.

[11] Brevik, I., and Bjørn, A., 1979. "Flume experiment on waves and currents. I. Rippled bed". *Coastal Engineering,* ***3***, pp. 149–177.

[12] Brevik, I., 1980. "Flume experiment on waves and currents II. Smooth bed". *Coastal Engineering,* ***4***, pp. 89–110.

[13] Thomas, G., 1981. "Wave-current interactions: an experimental and numerical study. Part 1. Linear waves". *Journal of Fluid Mechanics,* ***110***, pp. 457–474.

[14] Thomas, G., 1990. "Wave–current interactions: an experimental and numerical study. Part 2. Nonlinear waves". *Journal of Fluid Mechanics,* ***216***, pp. 505–536.

[15] Swan, C., Cummins, I., and James, R., 2001. "An experimental study of two-dimensional surface water waves propagating on depth-varying currents. Part 1. Regular waves".

Journal of Fluid Mechanics, ***428***, pp. 273–304.
[16] Umeyama, M., 2011. "Coupled piv and ptv measurements of particle velocities and trajectories for surface waves following a steady current". *Journal of Waterway, Port, Coastal, and Ocean Engineering,* ***137***(2), pp. 85–94.
[17] Kemp, P., and Simons, R., 1982. "The interaction between waves and a turbulent current: waves propagating with the current". *Journal of Fluid Mechanics,* ***116***, pp. 227–250.
[18] Swan, C., 1991. "An experimental study of waves on a strongly sheared current profile". In *Coastal Engineering 1990*. American Society of Civil Engineers, pp. 489–502.
[19] Umeyama, M., 2005. "Reynolds stresses and velocity distributions in a wave-current coexisting environment". *Journal of Waterway, Port, Coastal, and Ocean Engineering,* ***131***(5), pp. 203–212.
[20] Umeyama, M., 2009. "Changes in turbulent flow structure under combined wave-current motions". *Journal of Waterway, Port, Coastal, and Ocean Engineering,* ***135***(5), pp. 213–227.
[21] Chen, Q., Madsen, P. A., and Basco, D. R., 1999. "Current effects on nonlinear interactions of shallow-water waves". *Journal of Waterway, Port, Coastal, and Ocean Engineering,* ***125***(4), pp. 176–186.
[22] Choi, W., 2003. "Strongly nonlinear long gravity waves in uniform shear flows". *Physical Review E,* ***68***(2), p. 026305.
[23] Zhang, J. S., Zhang, Y., Jeng, D. S., Liu, P. L. F., and Zhang, C., 2014. "Numerical simulation of wave–current interaction using a RANS solver". *Ocean Engineering,* ***75***, pp. 157–164.
[24] Guyenne, P., 2017. "A high-order spectral method for nonlinear water waves in the presence of a linear shear current". *Computers & Fluids,* ***154***, pp. 224–235.
[25] Dalrymple, R. A., 1975. "Water waves on a bilinear shear current". In Coastal Engineering 1974, American Society of Civil Engineers, pp. 626–641, Copenhagen, Denmark. 24/06/1974–28/06/1974.
[26] Yoon, S. B., and Liu, P. L. F., 1989. "Interactions of currents and weakly nonlinear water waves in shallow water". *Journal of Fluid Mechanics,* ***205***, pp. 397–419.
[27] Hsu, H. C., Chen, Y. Y., Hsu, J. R. C., and Tseng, W. J., 2009. "Nonlinear water waves on uniform current in lagrangian coordinates". *Journal of Nonlinear Mathematical Physics,* ***16***(01), pp. 47–61.
[28] Duan, W., Wang, Z., Zhao, B., Ertekin, R., and Yang, W., 2018. "Steady solution of solitary wave and linear shear current interaction". *Applied Mathematical Modelling,* ***60***, pp. 354–369.
[29] Wang, Z., Zhao, B. B., Duan, W. Y., Ertekin, R. C., Hayatdavoodi, M., and Zhang, T. Y., 2020. "On solitary wave in nonuniform shear currents". *Journal of Hydrodynamics,* ***32***(4), pp. 800–805.
[30] Chen, H., and Zou, Q., 2019. "Effects of following and opposing vertical current shear on nonlinear wave interactions". *Applied Ocean Research,* ***89***, pp. 23–35.
[31] Kumar, A., and Hayatdavoodi, M., 2023. "Effect of currents on nonlinear waves in shallow water". *Coastal Engineering*, p. 104278.
[32] Chen, L. F., Zang, J., Hillis, A. J., Morgan, G. C. J., and Plummer, A. R., 2014. "Numerical investigation of wave-structure interaction using OpenFOAM®". *Ocean Engineering,* ***88***, pp. 91–109.
[33] Chen, L. F., Stagonas, D., Santo, H., Buldakov, E. V., Simons, R. R., Taylor, P. H., and Zang, J., 2019. "Numerical modelling of interactions of waves and sheared currents with a surface piercing vertical cylinder". *Coastal Engineering,* ***145***, pp. 65–83.
[34] Hirt, C. W., and Nichols, B. D., 1981. "Volume of fluid (vof) method for the dynamics of free boundaries". *Journal of Computational Physics,* ***39***(1), pp. 201–225.
[35] Ferziger, J. H., Perić, M., and Street, R. L., 2002. *Computational methods for fluid dynamics*, Vol. 3. Springer.
[36] Svendsen, I. A., and Jonsson, I. G., 1976. *Hydrodynamics of Coastal Regions*. Den Private Ingeniørfond, Technical University of Denmark.
[37] Rienecker, M. M., and Fenton, J. D., 1981. "A fourier approximation method for steady water waves". *Journal of Fluid Mechanics,* ***104***, pp. 119–137.
[38] Fenton, J. D., 1988. "The numerical solution of steady water wave problems". *Computers & Geosciences,* ***14***(3), pp. 357–368.
[39] Jacobsen, N., 2017. "waves2foam manual". *Deltares, The Netherlands*.
[40] Grue, J., 1992. "Nonlinear water waves at a submerged obstacle or bottom topography". *Journal of Fluid Mechanics,* ***244***, pp. 455–476.
[41] Hayatdavoodi, M., Ertekin, R. C., and Valentine, B. D., 2017. "Solitary and Cnoidal wave scattering by a submerged horizontal plate in shallow water". *AIP Advances,* ***7***(6), p. 065212.
[42] Kumar, A., and Hayatdavoodi, M., 2023. On wave-current interaction in deep and finite water depths. Accepted for publication in *Journal of Ocean Engineering and Marine Energy*.
[43] Hayatdavoodi, M., Seiffert, B., and Ertekin, R. C., 2015. "Experiments and calculations of Cnoidal wave loads on a flat plate in shallow-water". *Journal of Ocean Engineering and Marine Energy,* ***1***(1), pp. 77–99.
[44] Chen, L. F., Ning, D. Z., Teng, B., and Zhao, M., 2017. "Numerical and experimental investigation of nonlinear wave-current propagation over a submerged breakwater". *Journal of Engineering Mechanics,* ***143***(9), p. 04017061.
[45] Bracewell, R. N., 1989. "The Fourier transform". *Scientific American,* ***260***(6), pp. 86–95.